

Evidence for the Formation of 2:2 Drug–Mg²⁺ Dimers in Solution and for the Formation of Dimeric Drug Complexes on DNA from the DNA-Accelerated Photochemical Reaction of Antineoplastic Quinobenzoxazines

Hongtao Yu, Laurence H. Hurley, and Sean M. Kerwin*

Contribution from the Division of Medicinal Chemistry and Drug Dynamics Institute, College of Pharmacy, The University of Texas at Austin, Austin, Texas 78712-1074

Received January 26, 1996[⊗]

Abstract: The quinobenzoxazines are a group of topoisomerase II catalytic inhibitors that have demonstrated promising anticancer activity in mice. They have been proposed to form an unprecedented 2:2 drug–Mg²⁺ self-assembly complex on DNA. We have exploited the photochemical decomposition of the quinobenzoxazines to gain further support and insights into the nature of 2:2 quinobenzoxazine–Mg²⁺ dimers and the 2:2 drug–Mg²⁺ complex on duplex DNA. The quinobenzoxazine A-62176 undergoes photodecomposition to highly fluorescent products. Methyl viologen (MV²⁺) accelerates this photoreaction almost 500-fold. The formation of 2:2 drug–Mg²⁺ dimers in solution is deduced from the Mg²⁺-dependent difference in the MV²⁺-facilitated photoreaction rates of racemic and scalemic A-62176. However, both racemic and scalemic A-62176 have identical MV²⁺-facilitated photoreaction rates in the presence of Mg²⁺ and the achiral fluoroquinolone norfloxacin, due to heterochemical norfloxacin/A-62176 dimer complex formation. DNA also accelerates the photochemical decomposition of A-62176 up to 80-fold. This DNA-acceleration requires Mg²⁺, duplex DNA, molecular oxygen, and intercalation of the drug into the DNA duplex. In the proposed model for drug–DNA complexation, only one drug molecule of each 2:2 drug–Mg²⁺ dimer intercalates into the DNA duplex, the other molecule binds externally to the DNA. Norfloxacin, which can only play the external binding role, was able to modulate the photochemical reaction of the quinobenzoxazines on DNA. Furthermore, it appears that the precise positioning of the intercalated molecule, which is modulated by the structure and stereochemistry of the externally bound molecule, plays an important role in determining the rate of photoreaction on DNA. The implications of the observed photochemical reaction of the quinobenzoxazines are described for human phototoxicity, photodynamic therapy, mechanism of action studies, and improved drug design for both topoisomerase and gyrase inhibitors.

Introduction

The synthetic quinobenzoxazines are a new class of antineoplastic agents that are structural analogs of the antibacterial fluoroquinolones.^{1,2} Recent studies have shown that some quinobenzoxazine derivatives are active against a panel of human and murine tumor cell lines both *in vitro* and *in vivo* and have curative activity against solid tumors, murine tumors, and human tumor xenographs.^{1,3} While the antibacterial fluoroquinolones inhibit bacterial DNA topoisomerase II (gyrase)^{4–6} or IV^{7,8} activity by the formation of a “cleavable complex”, the quinobenzoxazines inhibit bacterial⁹ and mammalian¹⁰ topo-

isomerase II activity by a different mechanism. DNA binding studies reveal that the parent antibacterial quinolones do not bind duplex DNA but bind single-stranded DNA or the DNA–gyrase complex in the presence of Mg²⁺.^{11–15} In contrast, the quinobenzoxazines bind duplex DNA through intercalation in the presence of Mg²⁺, which bridges the phosphate backbone of the DNA and the β -ketoacid unit of the intercalated quinobenzoxazine.¹⁶ Furthermore, a drug self-assembly model has been proposed for the quinobenzoxazines in which a 2:2 drug–Mg²⁺ dimer binds DNA with one drug molecule intercalating between DNA base pairs and the other drug molecule externally bound through interactions with the DNA groove. Norfloxacin, an antibacterial fluoroquinolone which does not intercalate into duplex DNA, shows synergistic effects on the DNA binding of the quinobenzoxazines, suggesting that norfloxacin can replace the externally bound quinobenzoxazine of a DNA-bound 2:2 drug–Mg²⁺ complex.

* Address correspondence to this author. Telephone: (512)-471-5074. Fax: (512)-471-8664. e-mail: kerwin@erythrose.phr.utexas.edu.

[⊗] Abstract published in *Advance ACS Abstracts*, July 1, 1996.

(1) Chu, D. T. W.; Hallas, R.; Clement, J. J.; Alder, J.; McDonald, E.; Plattner, J. J. *Drugs Exptl. Clin. Res.* **1992**, *18*, 275–282.

(2) Chu, D. T. W.; Maleczka, R. E. *J. Heterocycl. Chem.* **1987**, *24*, 453–456.

(3) Clement, J. J.; Burren, N.; Jarvis, K.; Chu, D. T. W.; Swiniarski, J.; Adler, J. *Cancer Res.* **1995**, *55*, 830–835.

(4) Maxwell, A. *J. Antimicrob. Chemother.* **1992**, *30*, 409–414.

(5) Mitscher, L. A.; Shen, L. L. *Nucleic Acid Targeted Drug Design*; Propst, C. L., Perun, T. J., Eds.; Marcel Dekker, Inc.: New York, 1992.

(6) Willmott, C. J. R.; Critchlow, S. E.; Eperson, I. C.; Maxwell, A. *J. Mol. Biol.* **1994**, *242*, 351–363.

(7) Khodursky, A. B.; Zechiedrich, E. L.; Cozzarelli, N. R. *Proc. Natl. Acad. Sci. U.S.A.* **1995**, *92*, 11801–11805.

(8) Hoshino, K.; Kitamura, A.; Morrisey, I.; Sato, K.; Kato, J.-I.; Ikeda, H. *Antimicrob. Agents Chemother.* **1994**, *38*, 2623–2627.

(9) Kwok, Y.; Yu, H.; Kerwin, S. M.; Hurley, L. H. *Biochemistry*. To be submitted for publication.

(10) Permana, P. A.; Snapka, R. M.; Shen, L. L.; Chu, D. T. W.; Clement, J. J.; Plattner, J. J. *Biochemistry* **1994**, *33*, 11333–11339.

(11) Khac, S. B.-P.; Moreau, N. J. *J. Chromatogr. A* **1994**, *668*, 241–247.

(12) Shen, L. L.; Pernet, A. G. *Proc. Natl. Acad. Sci. U.S.A.* **1985**, *82*, 307–311.

(13) Shen, L. L.; Mitscher, L. A.; Sharma, P. N.; O'Donnell, T. J.; Chu, D. T. W.; Cooper, C. S.; Rosen, T.; Pernet, A. G. *Biochemistry* **1989**, *28*, 3885–3894.

(14) Shen, L. L. *Biochem. Pharmacol.* **1989**, *38*, 2042–2044.

(15) Shen, L. L.; Kohlbrenner, W. E.; Weigl, D.; Baranowski, J. *J. Biol. Chem.* **1989**, *264*, 2973–2978.

(16) Fan, J.-Y.; Sun, D.; Yu, H.; Kerwin, S. M.; Hurley, L. H. *J. Med. Chem.* **1995**, *38*, 408–424.

Here we describe studies in which we have taken advantage of the photoreaction of quinobenzoxazines to provide additional insights into the 2:2 drug–Mg²⁺ DNA complex. We have found that A-62176 is photoreactive in visible light. The photoreactivity of A-62176 is increased dramatically in the presence of the electron transfer mediator methyl viologen (MV²⁺). Differences in the photoreaction rates of racemic and scalemic A-62176 in the presence of MV²⁺ provide support for the formation of homochiral and heterochiral 2:2 drug–Mg²⁺ dimers in solution. Double-stranded DNA also serves to accelerate the photoreaction of A-62176. Furthermore, our studies of this photoreactivity of the quinobenzoxazines in the presence of the antibacterial fluoroquinolone norfloxacin provide further support and additional insights into our previously proposed quinobenzoxazine 2:2 drug–Mg²⁺ dimer complex with DNA.

Experimental Section

Materials and Instruments. The previously synthesized¹² quinobenzoxazine A-62176, [1-(3-aminopyrrolidin-1-yl)-2-fluoro-4-oxo-4H-quinol[2,3,4-*i,j*][1,4]-benzoxazine-5-carboxylic acid], was kindly provided by Abbott Laboratories, Abbott Park, IL. A-62176 was provided as both the *S* and *R* enantiomers as well as racemic material. As quinobenzoxazines are more soluble in acidic than neutral aqueous solution, stock solutions of A-62176 (0.5–1.0 mM) were prepared in 50 mM pH 2 sodium phosphate buffer. Concentrations of A-62176 solutions were determined spectrophotometrically using an extinction coefficient of $4.8 \times 10^4 \text{ M}^{-1} \text{ cm}^{-1}$ at 323 nm. Stock solutions of all other compounds were prepared by dissolving carefully weighed portions of drug into the appropriate solvent or buffer. Norfloxacin, ethidium bromide, and calf thymus DNA were purchased from Sigma and used without further purification. Methyl viologen chloride was purchased from Aldrich and used without further purification. All solvents were spectral grade. The calf thymus DNA concentration was determined by its absorbance at 260 nm with an extinction coefficient of 13 200 per mol of base pairs.¹⁷ Other DNA oligomers were synthesized by standard phosphoramidite chemistry on an automated synthesizer. Chromatography grade argon (Air Liquide) was deoxygenated by bubbling through a freshly prepared Fieser's solution (20 g of sodium thiosulfate, 5 g of anthraquinone, 100 g of KOH in 100 mL of water) followed by a saturated lead acetate solution.

Absorbance and Emission Spectra. Absorbance spectra were recorded on a Hewlett Packard HP 8452A diode array spectrophotometer. Fluorescence emission and excitation spectra were recorded on a Hitachi F-2000 fluorescence spectrophotometer. The excitation and emission monochromators were set at a width of 10 nm. Since the quinobenzoxazines are light sensitive, especially in the presence of DNA or MV²⁺, a shutter between the excitation light and the sample compartment was employed to minimize irradiation of the samples. Spectrophotometric titrations of enantiomeric (*S*- or *R*-)A-62176 were done essentially as described before for the racemic material.¹⁶

Kinetics and Rates for the Photochemical Reaction. Since the fluorescence emission maxima at 442 nm for the photoproduct of A-62176 is well separated from the emission maxima of the starting material quinobenzoxazine, ca. 505–520 nm, the intensity of the fluorescence emission at 420 nm was used to monitor the photoproduct formation. The buffers used in these studies were 20 mM phosphate, pH 7.5 with or without 2 mM MgCl₂. In the absence of added MgCl₂, 0.1 mM EDTA was added to chelate possible divalent cations. The light sources were either an 85 W Xe lamp (George W. Gates, Inc.) or the monochromatic excitation light beam from the F-2000 fluorescence spectrophotometer. The Xe lamp was placed 10 cm below a Pyrex glass plate with a stream of cool air blowing on the bottom of the glass to maintain the temperature. Samples (1 mL total volume) of quinobenzoxazine (10 μM) with varying concentrations of DNA in stoppered 10 × 10 × 35 mm quartz cuvettes were placed horizontally on top of the glass for desired irradiation time periods. The progress

of the photoreaction was monitored by directly measuring the fluorescence intensity at 420 nm for the photoproduct in the cuvettes after each period of irradiation. Three or more determinations were used to get an average value and standard deviation for the relative rates. For slower photoreactions, the measured F_{420} usually had a larger error because its change was small. For irradiations performed in the F-2000 fluorescence spectrophotometer, 0.5 mL of a 10 μM quinobenzoxazine solution were placed in a semimicro fluorescence cuvette (Uvonic, 4 × 10 × 35 mm, 10 mm excitation light path) sealed with a septum. Air or argon was bubbled through the reaction mixture by means of a short length of Teflon tubing that was threaded through the septum, with the end of the tubing positioned ca. 5–10 mm above the excitation light path. A needle through the septum was used as an outlet. In this way, the bubbling of air or argon through the cell ensured thorough mixing and, in the case of argon, anaerobic conditions. Anaerobic conditions were achieved by bubbling argon through the sample for 15 min before any measurements. The fluorescence intensity at 420 nm was recorded as a function of time during irradiation of the sample with the excitation beam (380 ± 10 nm). The initial reaction rate was calculated from the slope of the initial linear region of the plot. The experiments with added norfloxacin were done exclusively with 380 ± 10 nm light, where norfloxacin was not excited. We found that norfloxacin is also photoreactive with exciting light <350 nm (data not shown).

Molecular Modeling. Dimeric complexes of A-62176 with Mg²⁺ (2:2) were modeled in which the A-62176 molecules were either both of the same chirality (homochiral dimer) or each of a different chirality (heterochiral dimer). A slightly distorted octahedral coordination geometry about magnesium was assumed, in which each A-62176 molecule coordinates a different magnesium through its ketoacid moiety. The aminopyrrolidine amino group of each A-62176 molecule coordinates the magnesium atom that is coordinated by the ketoacid group of the other A-62176 molecule. This provides each of the two magnesium atoms a partial elongated octahedral coordination sphere consisting of two equatorial ligands (the ketoacid groups) and one axial ligand (the amino groups). The remaining three ligand sites around each metal atom were filled with water molecules. The bond lengths and angles involving coordination atoms were constrained using average crystal structural data for Mg.¹⁸ Bond lengths: Mg–O (carbonyl), 2.10 Å; Mg–O (carboxylate), 2.0 Å; Mg–N, 2.10 Å; Mg–O (water), 2.08 Å; with constants of 20 kcal/Å²·mol. Angles: All angles between coordination atoms were defined as 90° except for the angle between the carbonyl and carboxylate oxygen, which was 85°. The angle for Mg–O–H of the coordinated water molecules was 108°; for Mg–N–H and Mg–N–C of the amino group was 100° and 115°, respectively. All constants for angles were 0.1 kcal/mol·(deg)².

All unique configurational families were modeled for each dimer (10 families for the homochiral dimer and 12 families for the heterochiral dimer). These configurational families were generated by systematically varying the nature of overlay between the chromophores (wing-on-wing or overlapped, see later), the torsional angle about the C–N(aminopyrrolidine) bond (~0 or 180°), and the puckering of the aminopyrrolidine rings (amino group pseudoequatorial or pseudoaxial). With the exception of the coordination geometry about magnesium, which was constrained as discussed above, the starting configurations were minimized using the Tripos force field without charges. The lowest energy members from each configurational family for each dimer (homochiral or heterochiral) were then minimized without any constraints in PCModel (Serena Software, Bloomington, IN) using the MMX2 force field, in which explicit coordination about magnesium was defined.

Results

Ionic States, Absorption, and Emission Spectra of A-62176.

A-62176 has an amino and a carboxyl group that are ionizable in aqueous solutions. The pK_a values for these groups have not been determined, but those for the analogous quinolones are known. Generally, the pK_a for the carboxyl group ranges from 5.5–6.3.¹⁹ The primary amino group on the pyrrolidine ring should have a pK_a in the range of 9–10. Therefore, A-62176 should be primarily cationic in solutions of pH 5 and

(17) Mahler, H. R.; Kline, B.; Mehrotra, B. D. *J. Mol. Biol.* **1964**, *9*, 801–811.

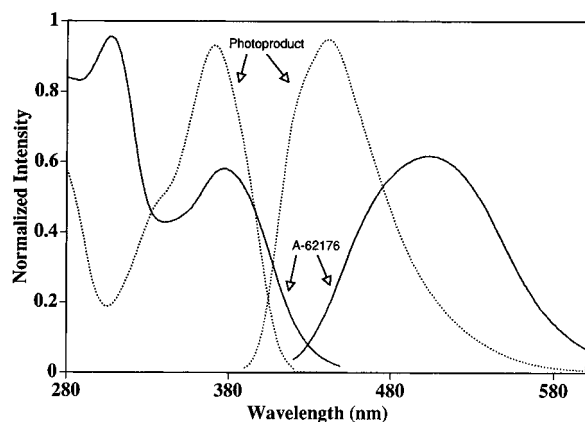


Figure 1. Normalized emission (right) and absorption (left) spectra of (RS)-A-62176 (solid line) and its photoproduct (dotted line).

lower and primarily zwitterionic in solutions of pH 7–8.5. At pH 7.5, (RS)-A-62176 displays two absorption bands at 314 and 385 nm. These two bands undergo bathochromic shifts to 323 and 390 nm, respectively, when the pH is lowered to 4. At pH 7.5, solutions of (RS)-A-62176 display a broad fluorescence emission that has a maximum at 510 nm, while at lower pH, a much weaker fluorescence peak at 525 nm is observed. Addition of excess calf thymus DNA and MgCl₂ shifts the emission slightly to the blue and increases the emission intensity more than three-fold (data not shown).

Photodecomposition of Quinobenzoxazines. A-62176 decomposes slowly in neutral aqueous solutions when exposed to room light. This is evidenced by changes in the fluorescence emission spectra. Freshly prepared solutions of A-62176 (10 μM, 20 mM phosphate buffer, pH 7.5) display a weak emission maxima at 510 nm. After standing for a few hours under ambient light, these same solutions display a new, intense emission maximum at 442 nm. Solutions of A-62176 kept in the dark show no change in fluorescence emission. Aqueous solutions of A-62176 at pH 2, and solutions of A-62176 in methanol, appear to be more stable to irradiation, as no changes in fluorescence emission are observed upon prolonged exposure to ambient light (data not shown).

The photochemical reaction of (RS)-A-62176 was studied by irradiating a solution of the drug in pH 7.5 phosphate buffer using a 85 W Xe lamp light source filtered through Pyrex glass. Fluorescence emission spectra were recorded after various irradiation times. The fluorescence emission of the drug solution displays the same changes as noted above, namely a hypsochromic shift in the emission band accompanied by an increase in emission intensity [Figure 1]. After a total of 10 h of irradiation under these conditions, the fluorescence intensity increases almost 20-fold, and no further changes are observed in the fluorescence spectrum upon further irradiation. Along with the changing emission spectrum, the absorption spectrum also shows significant changes [Figure 1] after irradiation. The two absorption bands with maxima at 314 and 385 nm for (RS)-A-62176 diminish in intensity as a result of irradiation, and a new absorption band with a maximum at 375 nm and a shoulder at 355 nm appears. These large spectral changes are indicative of the formation of one or more photoproducts as a result of irradiation of A-62176 with visible light. Using the fluorescence intensity at 420 nm, where the unreacted A-62176 displays only very weak emission, and where the photoproduct(s) display intense fluorescence emission, the progress of the photoreaction could easily be monitored.

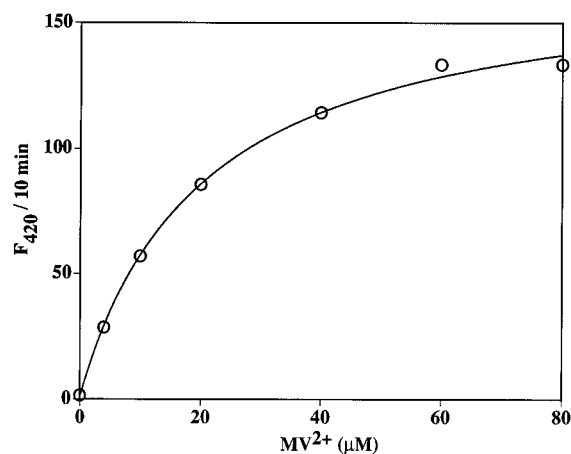


Figure 2. The photoreaction rate of (RS)-A-62176 expressed as the increase in the fluorescence intensity at 420 nm after 10 min of irradiation ($F_{420}/10$ min) versus the concentration of added methyl viologen (MV^{2+}). Continuously aerated solutions of (RS)-A-62176 (10 μM) in sodium phosphate buffer (20 mM, pH 7.5) containing 2 mM MgCl₂ and various concentrations of methyl viologen were subject to irradiation in a fluorescence spectrophotometer using the excitation beam (380 ± 10 nm) as the light source, with continuous monitoring of the fluorescence intensity of the reaction mixture.

Methyl Viologen Facilitates the Photoreaction of (RS)-A-62176.

By facilitating electron transfer from the excited state of substrate molecules, viologens can enhance the overall rate of photochemical process that occur via electron transfer.^{20–24} In the presence of MV^{2+} , the changes in the fluorescence spectra of (RS)-A-62176 upon irradiation are identical to those observed upon irradiation of solutions of (RS)-A-62176 in the absence of MV^{2+} (data not shown); however, the rate of change of the fluorescence spectra as a function of irradiation time is much faster in the presence of MV^{2+} . The fluorescence emission intensity at 420 nm (F_{420}) was used to monitor the formation of photoproduct as solutions of (RS)-A-62176 were subjected to irradiation by the excitation beam (380 ± 10 nm) of the fluorescence spectrophotometer. In this way, the fluorescence intensity at 420 nm could be monitored continuously during irradiation. Ample mixing and, when necessary, deoxygenation of the samples were accomplished by sparging the solutions with air or deoxygenated argon. The photoreaction rates at various MV^{2+} concentrations were estimated from the fluorescence intensity at 420 nm after 10 min of irradiation ($F_{420}/10$ min).²⁵ The rate of the photoreaction of (RS)-A-62176 increases as the concentration of MV^{2+} is increased from 0 to 60 μM. At concentrations of MV^{2+} greater than 60 μM, there does not appear to be a corresponding increase in the photoreaction rate [Figure 2]. At MV^{2+} concentrations of 60 μM and higher, the photoreaction rate of (RS)-A-62176 is 280 times faster than in the absence of MV^{2+} .

(20) Brun, A. M.; Hubig, S. M.; Rodgers, M. A. J.; Wade, W. H. *J. Phys. Chem.* **1992**, *96*, 710–715.

(21) Douglas, P.; Waechter, G.; Mills, A. *Photochem. Photobiol.* **1990**, *52*, 473–479.

(22) Dunn, D. A.; Lin, V. H.; Kochevar, I. E. *Biochemistry* **1992**, *31*, 11620–11625.

(23) Sasaki, S.; Mizutani, H.; Kase, Y.; Arai, T.; Hamada, T. *Inorg. Chim. Acta* **1994**, *225*, 261–267.

(24) Szulbinski, W. *Inorg. Chim. Acta* **1995**, *228*, 243–250.

(25) Plots of F_{420} versus irradiation time for these photoreactions in the presence of MV^{2+} demonstrate an initial lag period varying between 0 and 4 min, during which time the F_{420} increases relatively slowly with time [Figure 3]. Following this lag period, the plots of F_{420} versus time are nearly linear up to 30 min of irradiation, the longest irradiation time examined. Similar results to those in Figure 2 are obtained when the rate during the initial linear region (6–10 min) is plotted vs the MV^{2+} concentration (data not shown).

(18) Holloway, C. E.; Melnik, M. *J. Organomet. Chem.* **1994**, *465*, 1–63.

(19) Ross, D. L.; Riley, C. M. *Int. J. Pharm.* **1990**, *63*, 237–250.

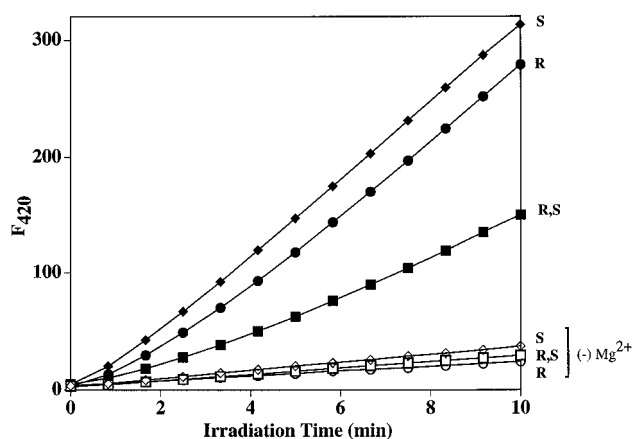
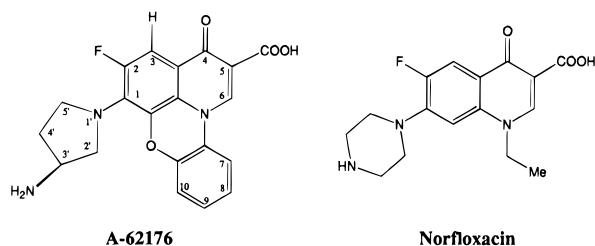


Figure 3. Methyl viologen-accelerated photoreaction rates of (*R*)-, (*S*)-, and (*RS*)-A-62176 (circles, diamonds, and squares, respectively) in the presence (filled symbols) or absence (open symbols) of 2 mM MgCl₂. Aerated solutions of racemic or scalemic A-62176 (10 μM) in sodium phosphate buffer (20 mM, pH 7.5) containing 80 μM MV²⁺ with or without added MgCl₂ (2 mM) were subject to irradiation in a fluorescence spectrophotometer using the excitation beam (380 ± 10 nm) as the light source. The amount of photoproduct formed was determined directly from the intensity of the 420 nm fluorescence as a function of the time of irradiation.

Effect of Optical Purity on the Photoreaction Rate of A-62176. Solutions of racemic, *R*-, and *S*-enantiomers of A-62176 in the presence of 80 μM MV²⁺ and 2 mM MgCl₂ in phosphate buffer, pH 7.5, were irradiated in the fluorescence spectrophotometer, as described above. The photochemical reaction rates for both pure *R*- and *S*-enantiomers of A-62176 are the same, within experimental error, but the rate of photoreaction of (*RS*)-A-62176 is nearly one-half the rate for the scalemic material [Figure 3]. The relative rates for the racemic mixture, *R*-, and *S*-enantiomers of A-62176 are respectively 280-, 480-, 490-fold faster in the presence of 80 μM MV²⁺ than the photoreaction rate of (*RS*)-A-62176 in phosphate buffer, 2 mM MgCl₂, pH 7.5, without added MV²⁺, as shown in Table 1. When racemic or scalemic A-62176 is irradiated in the presence of 80 μM MV²⁺, but in the absence of added MgCl₂, the photoreaction rate is much slower [Figure 3]. This rate decrease is not due to added EDTA (0.1 mM to chelate any adventitious divalent ion present); irradiation of these same solutions after the addition of 3 mM MgCl₂ results in photoreaction rates very close to those observed in the presence of 2 mM MgCl₂. Strikingly, in the absence of added MgCl₂, there is very little rate difference between racemic, *R*-, and *S*-enantiomers of A-62176 [Figure 3, Table 1].



Photoreaction of A-62176 in the Presence of Norfloxacin.

The effect of added norfloxacin on the irradiation of racemic or scalemic A-62176 in the presence of both MgCl₂ and MV²⁺ under the conditions described above was studied. Addition of 10 μM norfloxacin to a solution containing 10 μM A-62176 in the presence of 80 μM MV²⁺ and 2 mM MgCl₂ has very little effect on the photoreaction rate of either the pure enantiomers or the racemic A-62176 (data not shown). How-

Table 1. Relative Photoreaction Rates of A-62176 Accelerated by MV²⁺ ^a

	+ 80 μM MV ²⁺ 0.1 mM EDTA	+ 80 μM MV ²⁺ 2 mM MgCl ₂	+ 80 μM MV ²⁺ 2 mM MgCl ₂ 100 μM norfloxacin
(<i>R</i>)-A-62176	50	480 ± 60	450
(<i>S</i>)-A-62176	80	490 ± 60	440
(<i>R,S</i>)-A-62176	70	280 ± 40	450

^a The photoreaction rates were relative to the photoreaction rate of A-62176 (10 μM) in pH 7.5 sodium phosphate buffer bubbled with air in the absence of MV²⁺.

ever, addition of 100 μM norfloxacin inhibits slightly the photoreaction of the pure *R*- and *S*-enantiomers of A-62176 (5–10%), but enhances the photoreaction rate of the racemic mixture by approximately 60% [Table 1]. As a result, the photoreaction rates of racemic, (*R*)-, and (*S*)-A-62176 in the presence of excess norfloxacin are indistinguishable.

Molecular Modeling of A-62176 Homo- and Heterochiral Dimers. In order to gain insights into the differences between homochiral (e.g., *R-R* and *S-S*) and heterochiral (*R-S*) A-62176-Mg²⁺ 2:2 dimers that might give rise to the observed differences in photochemical rates, the ground state conformations of the homochiral and heterochiral dimers were investigated using molecular mechanics calculations. We examined many conformations for each monomer. Each of these different monomer conformations can be assembled into homochiral or heterochiral 2:2 quinobenzoxazine–Mg²⁺ dimers in which the chromophores of the monomers are either overlapped or staggered (“wing-on-wing”), and the resulting dimers subjected to molecular dynamics and minimization. Conformers having lowest PC-Model energies for each dimer type are shown in Figure 4. Comparing the energies for all dimers (see supporting information), the lowest energy conformation of the heterochiral dimer is 0.41 to 0.64 kcal/mol lower than the lowest energy conformer of the homochiral dimer. The overlapped conformation of both the homochiral and heterochiral dimers is calculated to be more favorable than the wing-on-wing conformation. However, in the case of the homochiral dimer, the energy difference separating the lowest energy overlapped conformer from the lowest energy wing-on-wing conformer (~1 kcal/mol) is greater than the energy separating the lowest energy heterochiral overlapped conformation from the lowest energy wing-on-wing conformation (~0.2 kcal/mol).

DNA Accelerates the Photoreaction of Quinobenzoxazines. The effect of added calf thymus DNA on the photochemical reaction of (*RS*)-A-62176 was studied by irradiating solutions of the drug in pH 7.5 phosphate buffer containing varying concentrations of DNA. An 85 W Xe lamp was employed as light source, and the relative amount of photoproduct formed after 5 min of irradiation was measured by determining the fluorescence intensity of the reaction solution at 420 nm, *F*₄₂₀.²⁶ Initially, as the concentration of DNA is increased, the photoreaction rate increases; however, at higher concentrations of DNA, corresponding to a ratio of DNA/(*RS*)-A-62176 of about five, a maximal photoreaction rate is reached [Figure 5]. At these higher DNA concentrations, the photochemical rate is approximately 60 times faster than the rate in the absence of DNA.

Factors affecting the DNA-accelerated photoreaction rate of (*RS*)-A-62176 were determined [Table 2]. The addition of MgCl₂ in the absence of added DNA has little effect on the photoreaction rate of (*RS*)-A-62176. In the presence of 40 μM

(26) Monitoring *F*₄₂₀ every minute for the fastest reactions indicated that the increase in *F*₄₂₀ was linear with irradiation time for up to 30 min of irradiation, the longest irradiation time examined.

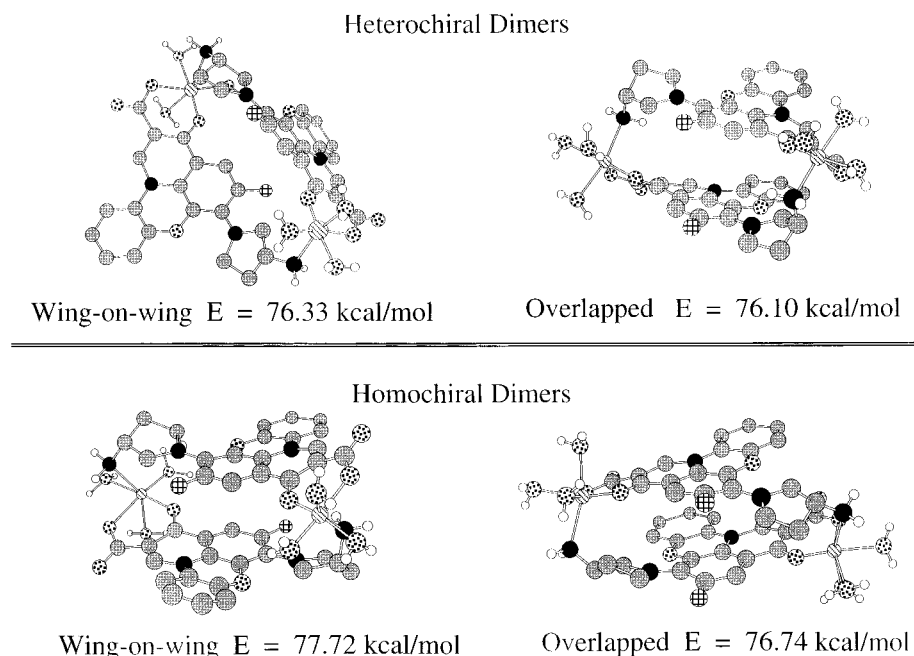


Figure 4. Structures and PCModel calculated energies for the lowest energy homochiral and heterochiral 2:2 A-62176-Mg²⁺ dimers. Both the lowest energy overlapped and wing-on-wing dimers are shown for the homochiral (*RR*) and heterochiral (*RS*) dimers.

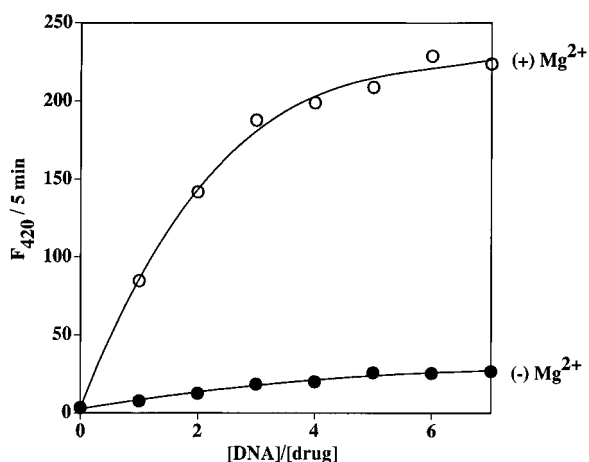


Figure 5. Rate of photoproduct formation from (*RS*)-A-62176, expressed as the intensity of the fluorescence at 420 nm after 5 min of irradiation ($F_{420}/5 \text{ min}$), as a function of added calf thymus DNA concentration, expressed as the ratio of the concentration of DNA base pairs to the initial concentration of (*RS*)-A-62176 ($[\text{DNA}]/[\text{drug}]$). Reaction solutions containing the indicated concentration of DNA and 10 μM (*RS*)-A-62176 (filled symbols) or 10 μM (*RS*)-A-62176 and 2 mM MgCl₂ (open symbols) were subjected to irradiation with an 85-W xenon lamp filtered with Pyrex glass.

Table 2. Relative Photoreaction Rate of A-62176^a

Mg ²⁺ , 2 mM	-	+	-	-	+	+	+
CT DNA, 40 μM	-	-	+	+	+	-	+
rel rates	1	1	5 \pm 1	5 ^b	50 \pm 10	2 ^c	13 \pm 3 ^d

^a All photoreactions were carried out in 20 mM sodium phosphate buffer (pH 7.5). The solutions of 1 mL A-62176 (10 μM) in a 3 mL quartz cuvette were irradiated with an 85-W xenon lamp at a distance of 10 cm through a Pyrex glass filter. Relative rates were determined by the fluorescence intensity of the photoproduct at 420 nm after 5 or 10 min of irradiation. ^b Addition of 4 mM KCl. ^c Using single-stranded oligomer d[GAAGAAAAG]. ^d Degassed by argon sparging for 15 min prior to irradiation.

DNA and 2 mM MgCl₂, the relative photoreaction rate of (*RS*)-A-62176 is 50-times faster than in the absence of DNA and MgCl₂. Elimination of MgCl₂ or replacement of MgCl₂ with 4 mM KCl in reaction solutions containing (*RS*)-A-62176 and 40

μM DNA results in a photoreaction rate which is only five times faster than the background rate, indicating the effect of added MgCl₂ on the DNA-accelerated photoreaction is not simply due to changes in the ionic strength of the medium.

To further explore the Mg²⁺ dependence of the relative photoreaction rate of A-62176 in the presence of DNA, (*RS*)-A-62176 (10 μM) and calf thymus DNA (40 μM) in phosphate buffer containing 0.1 mM EDTA were irradiated following the addition of varying amounts of MgCl₂. Under these conditions, addition of MgCl₂ increases the photoreaction rate, up to a concentration of 0.5 mM MgCl₂; thereafter further addition of MgCl₂ has no further effect on the photoreaction rate (data not shown). Therefore, the 2 mM MgCl₂ present in the preceding and following photochemical reactions of A-62176 is more than sufficient for achieving maximum photoreaction rate acceleration.

The photoreaction rate acceleration of A-62176 is greatest with double-stranded DNA. Irradiation of (*RS*)-A-62176 in the presence of the double-stranded oligomer [d(CGCGAATTCGCG)₂] affords a relative reaction rate that is nearly the same as that observed for irradiations performed in the presence of calf thymus DNA (data not shown). This eliminates the possibility that a minor protein contaminant present in the calf thymus DNA is responsible for the photoreaction rate acceleration. In contrast, addition of a single-stranded DNA oligomer d[GAAGAAAAG] (40 μM) to the photoreaction solution results in a relative rate that is only 2-fold faster than the rate observed in the absence of DNA, indicating that the rate acceleration due to double-stranded DNA is not merely a function of its polyanionic nature.

The DNA-accelerated photoreaction rate of (*RS*)-A-62176 is also oxygen facilitated. A reaction solution containing 10 μM quinobenzoxazine, 2 mM MgCl₂, and 40 μM calf thymus DNA in 20 mM phosphate buffer at pH 7.5 was bubbled with argon prior to irradiation. The resulting photoreaction rate was approximately one-fourth the rate obtained when no attempt was made to exclude oxygen [Table 2]. When the irradiation of A-62176 in the presence of DNA was carried out in the fluorescence spectrometer with continuous argon sparging, the

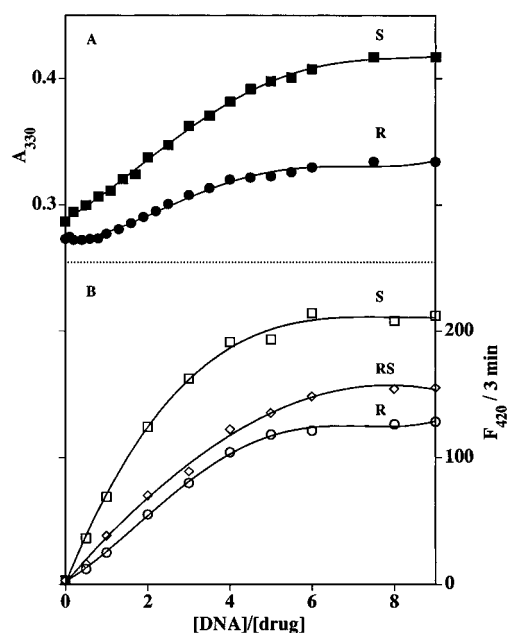


Figure 6. Effect of DNA concentration, expressed as the ratio of DNA concentration in base pairs to initial drug concentration ($[DNA]/[drug]$) on the absorbance at 330 nm (A, top) and relative photoreaction rate (B, bottom) for racemic (diamonds), (*R*-) (circles), and (*S*)-A-62176 (squares). Relative photoreaction rates for (*RS*-), (*R*-), and (*S*)-A-62176 (10 μM initial concentration) were determined as in Figure 5 and are expressed as the intensity of photoproduct fluorescence after 3 min of irradiation ($F_{420}/3 \text{ min}$).

photoreaction rate is 5-fold lower than when the photoreaction solution is bubbled with air (data not shown).

Differences in DNA Binding and Photoreaction of A-62176 Enantiomers. The binding of (*R*-) and (*S*)-A-62176 to DNA was studied using UV titration. A-62176 displays two UV absorption bands at 314 and 385 nm. Upon addition of calf thymus DNA, the 314 nm band gradually disappears with the appearance of a band at 330 nm for both enantiomers. The 385 nm band shifts to about 400 nm for both enantiomers and becomes broader (see supporting information). Although neither enantiomer gives rise to titration curves with perfectly clear isobestic points, the *S*-enantiomer produces a titration curve in which the isobestic points are more well-defined.

The data for the UV titration curves for (*R*-) and (*S*)-A-62176 are summarized in Figure 6A, which focuses on the changes in the 330 nm absorbance of the drugs upon addition of DNA. The absorbance at 330 nm for both the *R*- and *S*-enantiomers increases as the $[DNA]/[drug]$ ratio increases and levels off at a $[DNA]/[drug]$ ratio of 4–6 [Figure 6A]. Careful examination of the A_{330} vs $[DNA]/[drug]$ plot for the *R*-enantiomer [Figure 6A] reveals that there may be two distinct binding modes at different ratios of $[DNA]/[drug]$: at $[DNA]/[drug]$ ratios between 0 and 1 only relatively small changes in the absorption spectrum of the *R*-enantiomer of A-62176 are observed, whereas at $[DNA]/[drug]$ ratios above 1, there is a more pronounced absorbance increase, culminating in saturation at $[DNA]/[drug]$ ratios above 4–5. In contrast, for the *S*-enantiomer of A-62176, the changes in absorbance upon addition of DNA appear to be more uniform throughout the range of $[DNA]/[drug]$ of 0–4 [Figure 6A].

The photoreaction rate is also different for the enantiomers of A-62176 when bound to DNA. Figure 6B shows a plot of the fluorescence intensity due to the photoproduct after 3 min of irradiation in the presence of various calf thymus DNA concentrations. It is clear that the *S*-enantiomer has a faster photoreaction rate than the *R*-enantiomer at the same DNA

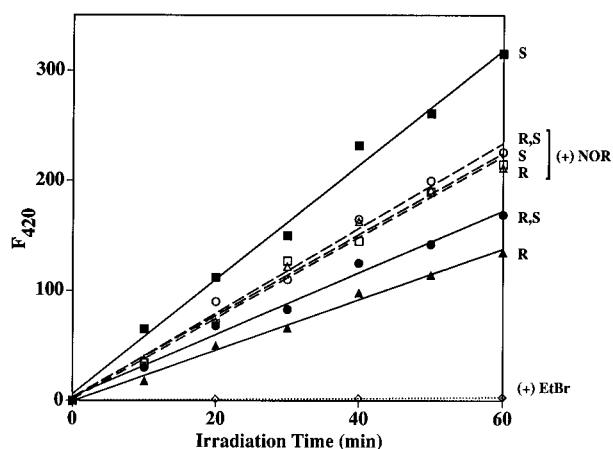


Figure 7. DNA-accelerated photoreaction progress, expressed as intensity of photoproduct fluorescence at 420 nm (F_{420}) as a function of irradiation time, for (*R*-), (*S*-), and (*RS*)-A-62176 (triangles, squares, and circles, respectively) alone (filled symbols), in the presence of norfloxacin (open symbols) or ethidium bromide (dotted line). Solutions of A-62176 (10 μM) in sodium phosphate buffer (20 mM, pH 7.5) containing 20 μM calf thymus DNA and 2 mM MgCl_2 and optionally containing either norfloxacin (10 μM) or ethidium bromide (10 μM) were subject to irradiation in a fluorescence spectrophotometer using the excitation beam ($380 \pm 10 \text{ nm}$) as light source. The photoreaction progress was followed by recording the intensity of the photoproduct emission at 420 nm as a function of irradiation time.

concentrations. Also reflected in Figure 6B is the biphasic nature of the DNA-accelerated photoreaction of the *R*-enantiomer; the initial slope of the F_{420} vs $[DNA]/[drug]$ ratio curve for the *R*-enantiomer is somewhat less than the slope at $[DNA]/[drug]$ ratios of 1–4. The photoreaction rate of the racemic mixture in the presence of DNA is intermediate between that observed for the *R*- and *S*-enantiomers. The maximal photoreaction rate for both the racemic and scalemic A-62176 levels off at a $[DNA]/[drug]$ ratio of about 5, which coincides with the $[DNA]/[drug]$ ratio that produces the maximal absorbance change at 330 nm for the titration [Figure 6A]. This correlation between the DNA binding and the DNA-accelerated photoreaction of these enantiomers indicate that the photoreaction rate acceleration is related to DNA binding.

DNA-Accelerated Photoreaction of A-62176 in the Presence of Norfloxacin. We have previously shown that addition of norfloxacin enhances the DNA binding ability of A-62176.¹⁶ The addition of 10 μM norfloxacin to the reaction solution of 10 μM A-62176 in the presence of 20 μM calf thymus DNA and 2 mM MgCl_2 also affects the photoreaction rate of scalemic and racemic A-62176. The photochemical reactions were conducted by using the monochromatic light from the excitation beam of the fluorescence spectrometer ($380 \pm 10 \text{ nm}$) with aeration of the samples. Figure 7 shows a plot of the F_{420} versus irradiation time of the photoreaction of A-62176. As shown, the *S*-enantiomer has the fastest photoreaction rate, followed by the racemic mixture, and the *R*-enantiomer. Addition of 10 μM norfloxacin accelerates the photoreaction of the *R*-enantiomer and the racemic mixture by 35 and 20%, respectively, but decreases the photoreaction of the *S*-enantiomer by 35%. In fact, in the presence of norfloxacin, the racemic and scalemic forms of A-62176 have similar DNA-accelerated photoreaction rates.

Addition of 10 μM ethidium bromide, an intercalator which competes with A-62176 for intercalation sites, decreases the DNA-accelerated photoreaction of A-62176 by 98% in all three cases. The photoreaction rate in the presence of ethidium bromide is nearly the same as the photoreaction rate of (*RS*)-A-62176 in the absence of DNA.

Discussion

The quinobenzoxazines are a structurally related group of fluoroquinolones that possess interesting topoisomerase II inhibitory and anticancer activities. Unlike the antibacterial fluoroquinolones, which do not appreciably bind double-stranded DNA, the quinobenzoxazines have been found to bind double-stranded DNA in a magnesium-dependent manner. The binding of quinobenzoxazines to DNA has been proposed to take place in a novel fashion involving the self-assembly on DNA of 2:2 drug–Mg²⁺ dimers. We have found that the quinobenzoxazines are photoreactive, and we have exploited the photochemical reactivity of quinobenzoxazines to study in more detail the proposed 2:2 drug–Mg²⁺ DNA complex.

Photodecomposition of Quinobenzoxazines. The quinobenzoxazine A-62176 photodecomposes slowly at neutral pH in water when left under ambient light. This photoreaction is easily monitored spectroscopically. As a result of the photoreaction, the two absorption bands at 314 and 385 nm due to the drug collapse into one band at 375 nm, and the weak fluorescence emission peak at 510 nm for the drug shifts to a strong emission peak at 442 nm [Figure 1]. Initial studies show that the photoreaction, as in the case of antibacterial quinolones,²⁷ produces rather complex photoproducts. Isolation and identification of these photoproducts is currently underway.

The Photoreaction of A-62176 May Involve Electron Transfer. The photodecomposition of A-62176 is accelerated in a concentration dependent fashion by MV²⁺. It is known that MV²⁺ is an electron mediator in many photosensitized,^{21–24} enzyme catalyzed,²⁸ and electrochemical^{29,30} reactions. In these reactions, MV²⁺ accepts an electron from a donor and itself becomes a cation radical (MV^{•+}). For the photosensitized reaction of A-62176, MV²⁺ probably accepts an electron from the excited state of A-62176, producing cation radicals of both MV²⁺ and the quinobenzoxazine. Under aerobic conditions, MV²⁺ is presumably regenerated from the cation radical MV^{•+} by O₂. The cation radical of the quinobenzoxazine formed from the MV²⁺ catalyzed photoreaction must go on to produce the same photoproduct(s) as those formed in the absence of MV²⁺. This implies that even in the absence of MV²⁺, the photoreaction of A-62176 proceeds through electron transfer from the excited state of the quinobenzoxazine.

Evidence for 2:2 A-62176–Mg²⁺ Dimers in Solution: Photoreaction Rate Differences of Racemic and Scalemic A-62176 in the Presence of Mg²⁺. Surprisingly, the MV²⁺-facilitated photoreaction of the pure *R*- or *S*-enantiomers of A-62176 is almost twice as fast as that of the racemic compound. In the absence of magnesium, the MV²⁺-accelerated photoreaction rates for racemic and scalemic A-62176 are nearly equal. Since MV²⁺ is not chiral, this difference in photoreaction rates can only be exhibited if the chiral drug is involved in intermolecular interactions with itself in the presence of Mg²⁺. In this case, the racemic drug may form diastereomeric ensembles in which a drug molecule of one chirality can interact with a drug of the same or opposite chirality. The observed rate differences would then be a consequence of the different photochemical rates associated with the ensemble consisting of drugs of all the same handedness versus the ensemble consisting of drugs of different handedness. Quinolones have been shown

to interact with various di- and trivalent metals to form dimers or multimers with drug:metal stoichiometries of 1:1, 2:1, or 3:1, depending on the particular drug and metal ion examined.^{31,32} Previously, we determined that the overall stoichiometry of the A-62176–Mg²⁺ complex is 1:1; however, we could not distinguish situations in which the actual ratio of A-62176 molecules to Mg²⁺ ions in the complex is 2:2 or higher. The observed difference in photoreaction rates for racemic and scalemic A-62176 is a strong indication that the A-62176 to Mg²⁺ ratio is 2:2 or higher. Considering the low drug concentrations employed in these studies (10 μM), the 2:2 dimer should be favored over higher equimolar (e.g., 3:3 etc.) drug–Mg²⁺ ensembles.

Because drug–Mg²⁺ dimer formation requires Mg²⁺, elimination of Mg²⁺ should eliminate the differences in the photoreaction rate of racemic and scalemic A-62176 due to dimer formation. In fact, under Mg²⁺-free conditions, there is almost no difference in the photoreaction rates of racemic and scalemic A-62176 [Figure 3]. This observation strongly supports the role of 2:2 drug–Mg²⁺ dimer formation in the observed difference in photoreaction rates for racemic versus scalemic A-62176 observed in the presence of Mg²⁺. Other interactions that might give rise to the observed rate differences in the presence of Mg²⁺, such as nonspecific drug aggregation or differences in the rate of reaction of an excited state A-62176 molecule with another A-62176 of the same or difference handedness, would be expected to be independent of the presence or absence of Mg²⁺.

The ratio of homochiral versus heterochiral 2:2 drug–Mg²⁺ dimers formed in solutions of the racemic drug should depend on the stability of each type of dimer. Molecular modeling indicates that the heterochiral dimer is slightly lower in energy (0.4–0.6 kcal/mol) than the homochiral dimer. Based on these enthalpic estimates, in solutions of racemic A-62176 containing Mg²⁺, there will be a preponderance of the heterochiral dimer over the homochiral dimer. If the homochiral dimer has a faster photoreaction rate than the heterochiral dimer, the preponderance of the latter in solutions of racemic A-62176 could explain the observed differences in the photoreaction rate. Although the origin of the difference in photoreaction rates between the homochiral and heterochiral dimers remains uncertain, the increased propensity of the homochiral dimers for overlapped conformations may play a role.

Photoreaction of A-62176 in the Presence of Norfloxacin: 2:2 Drug–Mg²⁺ Heterodimers of Quinobenzoxazine and Norfloxacin. The 2:2 drug–Mg²⁺ dimer motif should not be unique to quinobenzoxazines. Other fluoroquinolones, such as norfloxacin, should be able to form 2:2 drug–Mg²⁺ dimers and to replace one of the quinobenzoxazines in a 2:2 dimer to form a heterodimer consisting of one norfloxacin, one quinobenzoxazine, and two Mg²⁺ ions. Since norfloxacin is achiral, the resulting quinobenzoxazine–norfloxacin heterodimers formed in solutions of racemic A-62176 are enantiomeric and should have the same MV²⁺-facilitated photoreaction rate. In fact, in the presence of excess norfloxacin, the photochemical reaction rates of racemic and scalemic A-62176 are indistinguishable [Table 1]. Photolysis experiments in which the concentration of norfloxacin was equal to the concentration of A-62176 also resulted in a decrease in the photoreaction rate of the scalemic A-62176 and an increase in the rate of the photoreaction of the racemic A-62176. However, under these conditions, the photoreaction rate of the racemic A-62176 was still somewhat

(27) Tieffenbacher, E.-M.; Haen, E.; Przybilla, B.; Kurz, H. *J. Pharm. Sci.* **1994**, *83*, 463–467.

(28) Thanos, I.; Bader, J.; Günther, H.; Neumann, S.; Krauss, F.; Simon, H. *Methods Enzymol.* **1987**, *136*, 302–317.

(29) Douglas, P.; Mason, R. S.; Mills, A.; Russel, T. N.; White, M. V. *J. Phys. Chem.* **1992**, *96*, 816–819.

(30) Takenaka, S.; Ihara, T.; Takagi, M. *J. Chem. Soc., Chem. Commun.* **1990**, 1485–1487.

(31) Ross, D. L.; Riley, C. M. *Inter. J. Pharm.* **1993**, *93*, 121–129.

(32) Riley, C. M.; Ross, D. L.; Vander Velde, D.; Takusaagawa, F. *J. Pharm. Biomed. Anal.* **1993**, *11*, 49–59.

slower than that of the scalemic material, presumably due to the presence of some remaining diastereomeric A-62176 homodimers in the absence of an excess of added norfloxacin.

Insights into the Proposed Model of (A-62176–Mg²⁺)₂ on DNA Gained from Photochemical Studies. Previously we proposed that the (A-62176–Mg²⁺)₂ dimer complex binds DNA with one A-62176 molecule intercalating between DNA base pairs and the second binding externally through interactions with the DNA groove.¹⁶ The Mg²⁺ bridges the β -ketoacid unit of A-62176, the phosphate backbone of DNA, and the 3'-amino group of the partner A-62176 molecule in the intercalation complex. In the absence of Mg²⁺ there is no such complex formed, and only weak interactions between quinobenzoxazine and DNA exist. The drug dimers formed with Mg²⁺ in solution at micromolar concentrations found in this study certainly support the idea that the drug dimer is formed on DNA as well. Here we offer further photochemical evidence that support and offer further insights into this unique DNA binding mode of the quinobenzoxazines.

A Specific Intercalation Complex between A-62176 and DNA Is Responsible for the Photoreaction Rate Acceleration.

The irradiation of solutions at A-62176 and MgCl₂ containing calf thymus DNA results in the formation of photoproducts of A-62176 at a significantly faster rate than in the absence of DNA [Table 2]. The magnitude of this DNA-dependent photochemical rate acceleration is sensitive to the presence of Mg²⁺. In the absence of Mg²⁺, the addition of DNA causes only a modest increase (up to 8-fold) in the photoreaction rate of (*RS*)-A-62176, while in the presence of Mg²⁺, the DNA-dependent rate acceleration is as much as 60-fold for (*RS*)-A-62176 [Figure 5] and as much as 80-fold for (*S*)-A-62176 [Figure 6B]. As we have previously shown, the DNA binding of (*RS*)-A-62176 is Mg²⁺ dependent.¹⁶ In the absence of Mg²⁺, weak, nonspecific interactions between A-62176 and DNA may play a role in accelerating the photoreaction, but to a much lesser extent than that observed in the presence of Mg²⁺. Similarly, since the intercalation complex between (*RS*)-A-62176 and DNA cannot be formed with single-stranded DNA, the photochemical rate acceleration upon the addition of single-stranded DNA to solutions of A-62176 is much less than that with added double-stranded DNA.

Enantioselectivity on DNA Binding and on the Photoreaction of DNA-Bound A-62176. Additional support for the role of DNA binding in the photochemical rate acceleration due to DNA is obtained from comparing the effects of the stereochemistry of A-62176 on DNA binding and the DNA-accelerated photoreaction. As shown in Figure 6, the effect of DNA concentration on the photoreaction rates of (*R*)- and (*S*)-A-62176 are mirrored in changes in the UV–vis spectra of these compounds upon the addition of DNA. The initial photoreaction rate of racemic and scalemic A-62176 increases with increasing DNA concentration and levels off at a [DNA]/[A-62176] ratio of about 5, which corresponds to the same saturation ratio observed in the UV–vis titration. The photoreaction rate acceleration for the (*R*)-isomer of A-62176 is less than that for the (*S*)-isomer, which corresponds to the magnitude of changes in the UV–vis spectra of these two isomers upon addition of DNA. Finally, for the (*R*)-isomer of A-62176, there appears to be a region at low [DNA]/[drug] concentrations at which the photoreaction rate is relatively unaffected by DNA, which is mirrored in the UV–vis titration as a region of low DNA concentration at which there is little change in the 330 nm absorption of this isomer [Figure 6].

Photoreaction of a Heterodimeric Quinobenzoxazine–Norfloxacin 2:2 Drug–Mg²⁺ Dimer on DNA. We have

previously shown that norfloxacin and quinobenzoxazines display synergistic effects on binding to DNA.¹⁶ Here, we have presented evidence that norfloxacin can form heterodimeric complexes with A-62176 in solution. It appears reasonable that the synergistic effects of norfloxacin are due to its ability to form heterodimeric complexes with quinobenzoxazines on DNA. Although norfloxacin does not intercalate into duplex DNA, it could replace the externally bound A-62176 molecule in the quinobenzoxazine dimer complex on DNA. The thus liberated A-62176 may intercalate into DNA as quinobenzoxazine homodimers or as another heterodimeric complex with norfloxacin. Under these conditions, there is a shift in the proportion of quinobenzoxazine molecules that are intercalated relative to those quinobenzoxazine molecules that are bound externally.

For both the racemic mixture and the (*R*)-isomer of A-62176, the DNA-accelerated photoreaction rate in the presence of norfloxacin is faster than in the absence of norfloxacin. This clearly indicates that of the two functionally distinct quinobenzoxazine molecules in the complex of the 2:2 drug–Mg²⁺ dimer with DNA, it is the intercalated quinobenzoxazine that experiences the photoreaction rate acceleration. Interestingly, there is a decrease in the photoreaction rate of (*S*)-A-62176 in the presence of norfloxacin when compared to the rate in the absence of norfloxacin. The net result is that upon addition of 10 μ M norfloxacin, the DNA-accelerated photoreaction rates of racemic and scalemic A-62176 are indistinguishable. These results mirror exactly the results obtained for the MV²⁺-accelerated photoreaction of racemic and scalemic A-62176 in the presence of norfloxacin: The addition of norfloxacin causes previously kinetically distinguishable diastereomeric complexes to become kinetically indistinguishable. In the case of the DNA-accelerated photoreaction, one would expect that the enantiomeric heterodimeric A-62176–norfloxacin complexes would still exhibit different photoreaction rates on DNA. The fact that we cannot distinguish the photoreaction rates of these complexes may simply be due to the fact that they undergo photoreaction at rates that are very similar, although not necessarily identical. This indicates that the magnitude of photoreaction rate acceleration due to DNA for these 2:2 dimers may be dictated primarily by the nature of the externally bound molecule. This is akin to the steering effect of the minor-groove recognition motifs of certain major groove DNA-alkylating threading intercalators,³³ in that the positioning of the intercalated chromophore and alkylating moiety is controlled by the nature of the minor groove binding moiety. For enantiomeric A-62176 molecules, the achiral externally bound norfloxacin may control the positioning of the intercalated quinobenzoxazine, and therefore the photoreaction rate, irrespective of the handedness of the intercalated quinobenzoxazine.

In contrast to the results obtained with norfloxacin, addition of an intercalator, such as ethidium bromide, which can compete with A-62176 for intercalation sites, arrests any DNA-dependent photoreaction rate acceleration of A-62176.

Mechanism of the DNA-Accelerated Photoreaction of Quinobenzoxazines. The ability of MV²⁺ to facilitate the photoreaction of A-62176 leads us to postulate that the photoreaction of the quinobenzoxazines observed here results from electron transfer from the excited quinobenzoxazine to a receptor. In the absence of MV²⁺, the nature of the electron receptor is uncertain, but molecular oxygen is a likely candidate. We have observed that the rate of photoreaction of quinobenzoxazines is greatly decreased when the photolysis reactions are purged with argon [Table 2].

(33) Sun, D. K.; Hansen, M.; Hurley, L. H. *J. Am. Chem. Soc.* **1995**, *117*, 2430–2440.

The role that DNA plays in facilitating the photoreactions of quinobenzoxazines is not entirely clear. As the quinobenzoxazines bind DNA, the DNA-bound and the free molecules may display different physical properties and chemical reactivity. There are several classes of compounds whose chemical reactivity are changed due to DNA binding, such as CC-1065,³⁴ platinum(II) antitumor antibiotics,^{35–39} benzo[*a*]pyrene derivatives,^{40,41} dynemicin A,⁴² and various DNA reactive agents.^{22,43–46} In the case of (+)-CC-1065, the cyclopropyl ring of the drug is stable to nucleophiles at neutral pH in aqueous solution, but its reaction toward the N-3 of adenine is accelerated $>10^{10}$ times at specific DNA bonding sites.³⁴

Although the magnitude of the quinobenzoxazine DNA-photochemical rate acceleration studied here is on a more modest scale when compared to the rate acceleration demonstrated for (+)-CC-1065, the origin of the rate acceleration due to DNA may be similar in both cases. In the case of CC-1065, the large rate acceleration is due to a water molecule that plays a key role in facilitating the reaction and which is jointly positioned by the drug and the DNA phosphate groups.³⁴ In the case of the quinobenzoxazines, the externally bound drug molecule may play an important role in facilitating photoreaction. As discussed above, there may be a steering effect due to the externally bound quinobenzoxazine that affects the relative position of the intercalated quinobenzoxazine with respect to the DNA base pairs, and therefore the degree of π -stacking.

Implications for Drug Design. The quinobenzoxazines examined here, like some clinically important antibacterial fluoroquinolones,^{27,47–49} are sensitive to light irradiation under physiological conditions. The parent antibacterial fluoroquinolones are known to be phototoxic^{47,48,50,51} and to undergo photochemical reaction.^{27,49,52} The observation of quinobenzoxazine photoreactivity likewise has implications for the potential side effects for these compounds, which have been suggested as potential anticancer agents. Additionally, the facility of the photoreaction of the quinobenzoxazines studied

here, especially in the presence of DNA or electron acceptors, indicates that solutions of these compounds must be protected from visible light. Alternatively, the photoreactivity of the quinobenzoxazines may be beneficially applied in photodynamic therapy, especially considering the recent observation that the DNA-accelerated photoreaction of these compounds results in the cleavage of DNA.⁵³

By studying the photoreaction of the quinobenzoxazines, we have gained some important insights into our previously proposed model for the interaction of these compounds with Mg^{2+} and DNA. The Mg^{2+} -dependent differences in the photoreaction rates of scalemic and racemic A-62176 can best be explained by the formation of 2:2 drug– Mg^{2+} dimers, even in the relatively dilute drug solutions studied here. The self-assembly of these preformed 2:2 drug– Mg^{2+} dimers on DNA then provides a basis for the biological action of these drugs (topoisomerase II inhibition) as well as the DNA-accelerated photoreaction studied here. In the quinobenzoxazine 2:2 drug– Mg^{2+} dimer complex with DNA, the two quinobenzoxazine molecules play dissimilar roles, in that one quinobenzoxazine is intercalated, while the other quinobenzoxazine is bound externally to the DNA. This functional distinction of the two quinobenzoxazine molecules involved in the 2:2 drug– Mg^{2+} dimer complex with DNA is also reflected in the photoreaction studied here, in that only the intercalated quinobenzoxazine experiences a substantial DNA-dependent photoreaction rate acceleration. Furthermore, the functional distinction between the two drug molecules in the DNA-bound dimer may mimic the bipartite nature of known topoisomerase II inhibitors, such as amsacrine, which possesses a DNA intercalating moiety (acridine) and a group (phenylsulfonamide) that is thought to interact specifically with the topoisomerase enzyme.⁵⁴ Clearly, in the case of the quinobenzoxazines, separately optimizing each of these two molecules for these two distinct roles should result in a more potent and selective topoisomerase II inhibitor.

The ability of heterodimeric quinobenzoxazine–norfloxacin 2:2 drug– Mg^{2+} complexes to undergo DNA-accelerated photoreaction, and our recent observation that the DNA-accelerated photoreaction of quinobenzoxazines is accompanied by DNA strand scission,⁵³ leads to the possibility that the quinobenzoxazines could be used to map the fluoroquinolone DNA binding sites in the tertiary fluoroquinolone– Mg^{2+} –DNA–gyrase or –topoisomerase II complexes. These studies are currently underway.

Acknowledgment. Support for this research through the Public Health Service (GM-50892 to S.M.K. and CA-49751 to L.H.H.) is gratefully acknowledged.

Supporting Information Available: Molecular modeling study of the quinobenzoxazine– Mg^{2+} dimers, PCModel energy for *R*–*R* and *R*–*S* dimers of A-62176, and spectral changes of (*R*)- and (*S*)-A-62176 upon addition of calf thymus DNA (6 pages). See any current masthead page for ordering and Internet access instructions.

JA9602859

(53) Yu, H.; Kwok, Y.; Hurlley, L. H.; Kerwin, S. M. *Biochemistry*. To be submitted for publication.

(54) Zwelling, L. A.; Mitchell, M. J.; Satitpunwaycha, P.; Mayes, J.; Altschuler, E.; Hinds, M.; Baguley, B. C. *Cancer Res.* **1992**, *52*, 209–217.

(34) Warpehoski, M. A.; Harper, D. E. *J. Am. Chem. Soc.* **1995**, *117*, 2951–2952.

(35) Anin, M.-F.; Gaucheron, F.; Leng, M. *Nucleic Acids Res.* **1992**, *20*, 4825–4830.

(36) Dalbies, R.; Payet, D.; Leng, M. *Proc. Natl. Acad. Sci. U.S.A.* **1994**, *91*, 8147–8151.

(37) Gaucheron, F.; Malinge, J.-M.; Blacker, A. J.; Lehn, J.-M.; Leng, M. *Proc. Natl. Acad. Sci. U.S.A.* **1991**, *88*, 3516–3519.

(38) Payet, D.; Gaucheron, F.; Sip, M.; Leng, M. *Nucleic Acids Res.* **1993**, *21*, 5846–5851.

(39) Sundquist, W. I.; Bancroft, D. P.; Chassot, L.; Lippard, S. J. *J. Am. Chem. Soc.* **1988**, *110*, 8559–8560.

(40) Geacintov, N. E.; Yoshida, H.; Ibanez, V.; Harvey, R. G. *Biochemistry* **1982**, *21*, 1864–1869.

(41) Michaud, D. P.; Gupta, S. C.; Whalen, D. L.; Sayer, J. M.; Jerina, D. M. *Chem.-Biol. Interact.* **1983**, *44*, 41–52.

(42) Myers, A. G.; Cohen, S. B.; Tom, N. J.; Madar, D. J.; Fraley, M. E. *J. Am. Chem. Soc.* **1995**, *117*, 7574–7575.

(43) Buckley, N. J. *J. Am. Chem. Soc.* **1987**, *109*, 7918–7920.

(44) Armitage, B.; Yu, C.; Devadoss, C.; Schuster, G. B. *J. Am. Chem. Soc.* **1994**, *116*, 9847–9859.

(45) Atherton, S. J.; Harriman, A. *J. Am. Chem. Soc.* **1993**, *115*, 1816–1822.

(46) Kohn, K. W.; Hartley, J. A.; Mattes, W. B. *Nucleic Acids Res.* **1987**, *15*, 10531–10549.

(47) Ferguson, J.; Johnson, B. E. *British J. Dermatology* **1993**, *128*, 285–295.

(48) Wainwright, N. J.; Collins, P.; Ferguson, J. *Drug Safety* **1993**, *9*, 437–440.

(49) Vagars, F.; Rivas, C.; Machado, R. *J. Photochem. Photobiol. B. Biol.* **1991**, *11*, 81–85.

(50) Halkin, H. *Rev. Infect. Dis.* **1988**, *10*(Suppl. 1), 258–262.

(51) Christ, W.; Lehnert, T.; Ulbrich, B. *Rev. Infect. Dis.* **1988**, *10*(Suppl. 1), 141–145.

(52) Iwamoto, Y.; Kurita, A.; Shimizu, T.; Masuzawa, T.; Uno, K.; Yagi, M.; Kitagawa, T.; Oku, T.; Yanagihara, Y. *Biol. Pharm. Bull.* **1994**, *17*, 654–657.